*Chinese Journal of*
**POLYMER SCIENCE**

ARTICLE

https://doi.org/10.1007/s10118-018-2155-2
*Chinese J. Polym. Sci.* 2018, 36, 1394–1402

# Mesoscopic Simulation Assistant Design of Immiscible Polyimide/BN Blend Films with Enhanced Thermal Conductivity

Guo-Dong Zhang[a,b], Lin Fan[a,b*], Lan Bai[a,b], Min-Hui He[a], Lei Zhai[a], and Song Mo[a]

[a] *Laboratory of Advanced Polymer Materials, Institute of Chemistry, Chinese Academy of Sciences, Beijing 100190, China*
[b] *School of Chemistry and Chemical Engineering, University of Chinese Academy of Sciences, Beijing 100049, China*

**Abstract** The mesoscopic simulation technique was applied to describe the phase separation behavior of polyimide blends and used for design of immiscible polyimide/BN blend films with enhanced thermal conductivity. The simulation equilibrium morphologies of different poly(amic acid) (PAA) blend systems were investigated and compared with optical images of corresponding polyimide blend films obtained by experiment. The immiscible polyimide blend films containing nano-/micro-sized BN with vertical double percolation structure were prepared. The result indicated that the thermal conductivity of polyimide blend film with 25 wt% nano-sized BN reached 1.16 W/(m·K), which was 236% increment compared with that of the homogenous film containing the same BN ratio. The significant enhancement in thermal conductivity was attributed to the good phase separation of polyimide matrix, which made the inorganic fillers selectively localized in one continuous phase with high packing density, consequently, forming the effective thermal conductive pathway.

**Keywords** Polyimide films; Boron nitride; Mesoscopic simulation; Thermal conductivity

**Citation:** Zhang, G. D.; Fan, L.; Bai, L.; He, M. H.; Zhai, L.; Mo, S. Mesoscopic Simulation Assistant Design of Immiscible Polyimide/BN Blend Films with Enhanced Thermal Conductivity. Chinese J. Polym. Sci. 2018, 36(12), 1394–1402.

## INTRODUCTION

Polyimide (PI) films have been widely used in electronic and electrical industries as insulating materials for flexible printed circuit boards, satellite solar cell panels, electric motors and transformers because of their high thermal stability, good mechanical and favorable electrical insulating properties[1–3]. However, the pure polyimide films are generally with intrinsic low thermal conductivity in the range of 0.1–0.2 W/(m·K), which cannot effectively dissipate the heat generated from high packing and power-density devices[4]. In order to solve the problem of heat dissipation, thermal conductive and electronically insulating ceramic fillers, such as alumina ($Al_2O_3$), aluminum nitride (AlN), boron nitride (BN), and silicon nitride ($Si_3N_4$), have been introduced to the polyimide matrix to form the composite films[5–9]. Many efforts have been made to develop the homogeneous polyimide composite films by incorporation of ceramic fillers in polymeric matrix. It is found that a high loading of inorganic fillers in the polymer matrix (in general over 30 wt%) is necessary for achieving high thermal conductivity, which is associated with the formation of continuous heat dissipation networks throughout the polymeric matrix. Unfortunately, the high fraction of fillers in polyimide composite films inevitably leads to poor processability and poor mechanical properties due to aggregation of inorganic fillers, as well as high cost.

Many other researches have been done on improving the thermal conductivity of polyimide films with less filler loading by introducing hybrid fillers or controlling filler distribution to construct effective thermal conductive networks[10, 11]. Hsu *et al*. reported their works on polyimide composite films containing micro- and nano-sized BN particles. They found that the thermal conductivity of the PI/BN film with micro-/nano-sized BN ratio of 7:3 at 30 wt% of filler loading achieved 1.2 W/(m·K) due to the formation a random conductive bridge or network[12]. Shoji *et al*. prepared BN composite films based on the cross-linked liquid crystalline (LC) polyimides[13]. They suggested that the vertically oriented cross-linked LC polyimides played an important role in the effective phonon conduction between BN and the matrix. The thermal diffusivity in the thickness direction of the composite films was 0.679 $mm^2/s$ at 30 vol% BN loading. In recent years, immiscible polymer blend films have attracted more attention because they exhibit higher thermal diffusivity alone the out-of-plane direction than the monophasic PI blend films[14–16]. Ando *et al*. prepared the immiscible polyimide blend films based on a sulfur- and a fluorine-containing PI with pyramidal-shaped zinc oxide (ZnO)[17, 18]. They claimed that the PI blend films exhibited microphase separated structures with a vertical double percolation morphology, in which two immiscible phases were separatedly aligned alone the out-of-plane direction and the ZnO particles were preferentially precipitated in the

* Corresponding author: E-mail fanlin@iccas.ac.cn
Received April 17, 2018; Accepted May 8, 2018; Published online June 12, 2018

fluorine-containing PI phase. The PI blend films gave the thermal conductivity as high as 1.54 W/(m·K) at 27 vol% of ZnO particles filling due to the effective thermal conductive pathway. However, the mass weight of ZnO particles in their PI blend films was nearly 59.1 wt%, which was still too high to obtain the polyimide films with reasonable mechanical properties.

In general, it is considered that the phase separation of polymer blends is related with their chemical structures. The resulting mesoscale morphology can be either the droplet-matrix or the double percolation structure, which further affects the thermal conductivity and mechanical properties of composite films in different ways. The mesoscale changes in the morphology of composite films determine the double percolation structure and further affect their thermal conductivity and mechanical properties. Therefore, it is necessary to clarify the correlation between the phase separation structure of immiscible polymer blend films and their high thermal conductivity.

In this research, the mesoscopic simulation technique was applied to describe the morphology of polyimide blends and used for design of immiscible polyimide/BN blend films with better vertical double percolation structure. In addition, the hexagonal BN is isostructural to graphene and considered to be an ideal choice in thermal and electrical applications due to its atomically flat and electrically insulating surface[19–21]. This mesoscopic simulation assistant research on phase separation behavior of polyimide blends might provide an effective method to direct the fabrication of polyimide composite films with high thermal conductivity at low filler loading. According to the simulation and experimental results on the phase separation behavior of polyamic acid (PAA) blend systems, the immiscible polyimide blend films containing different ratios of nano-/micro-sized BN were prepared. The morphology of the PI/BN blend films was investigated. Their thermal conductivity was discussed and compared with the homogenous ones.

## MODEL AND SIMULATION

The morphology of polyimide blend mainly depends on the property of its precursor—poly(amic acid) (PAA) due to the high viscosity. The macromolecular structures of PAA with different molecular volumes used in the simulations are shown in Fig. 1(a). For the initial simulation of solubility parameters ($\delta$) in Synthia module, the temperature and appropriate molecular weight were set as 298 K and 2.5 × $10^4$ g/mol, respectively. The molecular volume and solubility parameter of these polyamide acids are listed in Table 1. Flory-Huggins parameter $\chi$ was estimated using Eq. (1):

$$\chi_{ij} = \frac{V(\delta_i - \delta_j)^2}{RT} \quad (1)$$

where $V$ refers to the mean molar volume of PAA blends, while $\delta_i$ and $\delta_j$ represent the solubility parameters of the two kinds of PAA in the blend system, respectively. The Flory-Huggins parameters have a linear relationship with dissipative particle dynamics (DPD) repulsion parameters ($\alpha_{ij}$). This relationship could be used to obtain $\alpha_{ij}$ with a known $\chi_{ij}$ value. A single repeat unit of PMDA/ODA was chosen as the basic coarse-grained (CG) particle to construct polymer system as shown in Fig. 1(b)[22]. All the simulations were performed using Mesocite module in the Material Studio suite of programs. The structures of particles were optimized before set into Mesostructure Template. The dimensions of the simulation lattice were 300 Å × 300 Å × 300 Å, time step was 250 fs and the number of time steps was 8000.

The characteristic ratio of PMDA/ODA was 3.38, therefore, the bead mass was set as 1414 amu. The length scale determined from the bead size was 15.59 Å. The simulated density was set to the default value as $\rho$ = 3. The PAA blend systems of PAA2/PAA3, PAA3/PAA5, PAA4/PAA5, PAA2/PAA5 and PAA1/PAA5 were selected and their $\chi_{ij}$ values were in the increasing order and used to predict the repulsion parameters $\alpha_{ij}$. The parameters $\alpha_{ij}$ of different PAA blend systems can be calculated from Eq. (2).

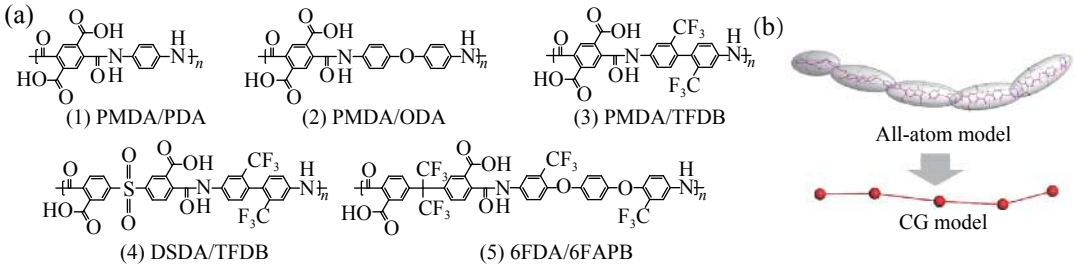


**Fig. 1** (a) Macromolecular structures of poly(amic acid)s in all-atom model; (b) Coarse-grained structure of PMDA/ODA

**Table 1** Molecular volume and solubility parameter of poly(amic acid)s

| Sample | Poly(amic acid) | Molecular volume ($cm^3$/mol) | Solubility parameter ($(J/cm^3)^{0.5}$) |
|---|---|---|---|
| PAA1 | PMDA/PDA | 230.14 | 29.14 |
| PAA2 | PMDA/ODA | 305.49 | 27.29 |
| PAA3 | PMDA/TFDB | 355.84 | 25.46 |
| PAA4 | DSDA/TFDB | 448.67 | 25.80 |
| PAA5 | 6FDA/6FAPB | 579.69 | 22.98 |

https://doi.org/10.1007/s10118-018-2155-2

$$\alpha_{ij} = 25 + 3.5\chi_{ij} \quad (2)$$

According to the parameters listed in Table 2, the morphology evolution and eventual phase separation could be examined.

**Table 2** Flory-Huggins parameters and repulsion parameters of PAA blend systems

| Sample | $\chi_{ij}$ | $\alpha_{ij}$ |
|---|---|---|
| PAA2/PAA3 | 0.45 | 26.58 |
| PAA3/PAA5 | 1.16 | 29.06 |
| PAA4/PAA5 | 2.43 | 33.51 |
| PAA2/PAA5 | 3.32 | 36.62 |
| PAA1/PAA5 | 6.20 | 46.70 |

## EXPERIMENTAL

### Materials

The dianhydrides of 1,2,4,5-benzenetetracarboxylic anhydride (Lonza), 3,3′,4,4′-diphenylsulfonetetracarboxylic dianhydride (DSDA, Tokyo Chemical Industry Co. Ltd.) and 4,4′-(hexafluoroisopropylidene)diphthalic anhydride (6FDA, Daikin Industries, Ltd., China) were dried in a vacuum oven at 120 °C for 12 h prior to use. The aromatic diamines of *p*-phenylenediamine (PDA, Amino-Chem), 4,4′-oxydianline (ODA, Shandong Wanda Chemical Co., China), 2,2′-bis(trifluoromethyl)benzidine and 1,4-bis(4-amino-2-trifluoromethyl phenoxy)benzene (TFDB and 6FAPB, Changzhou Sunlight Pharmaceutical Co., Ltd., China) were used as received. Commercially available *N*,*N*-dimethyl-acetamide (DMAc) was purified by vacuum distillation. Hexagonal boron nitride powders with platelet morphology and the particle size of 70 nm (nBN, Forsman Scientific Co.) and 2.7 μm (mBN, Beijing Zhongjinyan Material Co.), respectively, were used.

### Polymer Synthesis and Film Preparation

The pure poly(amic acid) (PAA) solution was synthesized by polycondensation of aromatic diamine and dianhydride in DMAc with stirring under nitrogen atmosphere at room temperature for 12 h. The molar ratio of diamine and dianhydride was 1:1. The solid content of PAA solution was kept at 20 wt%. The pure polyimide blend film was prepared by mixing two kinds of PAA solutions, stirring for 1 h, then casting on a glass substrate and successively heating in the procedure of 60 °C/2 h, 250 °C/1 h and 350 °C/1 h to complete the imidization. The immiscible polyimide blend films containing BN filler were prepared from the mixture of PAA2/BN and PAA5 solutions in the similar procedure as described above. Firstly, the PAA2/BN solution was prepared by dispersing the BN powder in DMAc with an ultrasonic device for 5 min, filling the mixture into a completely dried flask placed with diamine ODA, and adding dianhydride PMDA under stirring for 12 h. Then, the obtained PAA2/BN solution was mixed with pure PAA5 solution and stirred for 1 h. The immiscible polyimide blend film containing BN (PI2/PI5/BN) was obtained after casting the BN blended solution on a glass substrate followed by thermal imidization. A series of BN blended polyimide films with the mBN or nBN content of 5 wt%, 10 wt%, 15 wt%, 20 wt%, and 25 wt%, respectively, were prepared in the similar procedure. The films were 30–40 μm thick. Homogenous BN blended polyimide films were prepared from PAA2/BN solution for comparison.

### Characterization and Measurements

Optical images and 3D fluorescent images of polyimide films were taken with an Olympus IX83 microscope and a FV1000-IX81 confocal fluorescence microscope, respectively. Scanning electron microscopy (SEM) was performed on a Hitachi S-4800 scanning electron microscope using film samples coated with platinum. Raman spectra were recorded on a Bruker RFS 100/S spectrometer. Thermal conductivity was measured on a Hot Disk TPS 2500S thermal constants analyser. Mechanical properties were measured on Instron 3365 tensile apparatus with 120 mm × 10 mm specimens in accordance with GB1040-79 at a drawing rate of 50 mm/min.

## RESULTS AND DISCUSSION

### Phase Separation Behavior of Polyimide Blends

It is well known that the phase separation starts when the $\chi_{ij}$ or $\alpha_{ij}$ reaches a critical value. In order to gain an insight into the phase separation process, mesoscopic dissipative particle dynamics simulation was applied to describe interactions between different PAA blend systems. Both order parameters and equilibrium morphology could be obtained by this simulating method. The order parameters were used to represent the phase-separating ability, for which higher value indicates better phase separation structure[23]. Fig. 2 shows the time evolution of order parameters of different PAA blend systems, in which the two kinds of PAA solutions were in the equivalent weight ratio. The results indicated that the order parameters of these PAA blends could be divided into two stages with time evolution. During the first stage (I), the order parameters rapidly increased, implying the gradual change from an initial homogenous system to a fine system with a clear phase separation. Subsequently, the system reached equilibrium and the bulky two-phase morphology that spanned the whole sample in the second stage (II). The order parameters of different PAA blend systems had the following trend: PAA1/PAA5 ≈ PAA2/PAA5 > PAA4/PAA5 > PAA3/PAA5 > PAA2/PAA3.

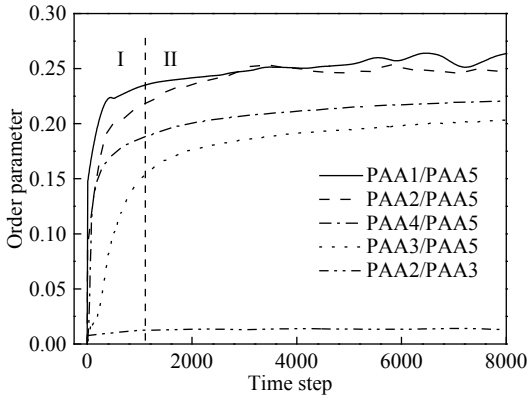


**Fig. 2** Time evolution of order parameters of different PAA blend systems

Further information concerning the influence of $\alpha_{ij}$ on phase separation of PAA blends could be obtained from the mesoscopic simulation and experimental results, which are illustrated in Fig. 3. In addition, mesoscopic simulation provided the visual evidence for the equilibrium morphology and the density field maps appearing with different $\alpha_{ij}$. According to the density maps, it could be concluded that the phase separation ability of PAA blends was significantly affected by degree of $\alpha_{ij}$. The strong phase separation occurred only at higher $\alpha_{ij}$[24–29]. For example, PAA2/PAA3 blends ($\alpha_{ij}$ = 26.58) had a vague density field boundary in the mesoscopic simulation. The similar phenomena were observed for both of PAA3/PAA5 ($\alpha_{ij}$ = 29.06) and PAA4/PAA5 ($\alpha_{ij}$ = 33.51) blends. With further increase of $\alpha_{ij}$, clear phase separation appeared. The density field maps for PAA2/PAA5 ($\alpha_{ij}$ = 36.62) and PAA1/PAA5 ($\alpha_{ij}$ = 46.70) revealed better separatrix. The PI blend films were prepared from the corresponding PAA blends after thermal imidization. The optical images of these PI blend films were detected and compared with the mesoscopic simulation results. It was found that only the PI blend films based on PAA2/PAA5 and PAA1/PAA5 blends exhibited sharp phase-separated morphology. The experimental results were consistent with the mesoscopic simulation ones.

The $\chi_{ij}$ or $\alpha_{ij}$ determined the separating ability of PAA blends, while the mass ratio also contributed to the equilibrium morphologies of polyimide blends. The influence of weight ratio of PAA2/PAA5 blend on the phase separation behavior was investigated. The weight ratio of PAA2/PAA5 was varied from 1:3, 1:1 to 3:1. As shown in Fig. 4, when the weight ratio of PAA2/PAA5 was varied 1:3, both the simulation and experimental results of polymer blend revealed a sea-island structure. The PAA2/PAA5 blend changed to a continuous structure as their weight ratio enhanced to 1:1. However, as the weight ratio of PAA2/PAA5 changed to 3:1, a sea-island structure appeared again. It was confirmed that the blend films prepared from the PAA blends with the equivalent weight ratio of components had continuous phase separation structure. However, the immiscible polyimide films are obtained when the thermal conductive fillers are incorporated. With the help of a good phase separation structure, the fillers can be selectively localized in one continuous phase with high density and consequently form an effective thermal conductive pathway.

The three-dimensional (3D) morphology of PI2/PI5 blend film was examined by an FV1000-IX81 confocal fluorescence microscope[30, 31]. This method enables us to image consecutively 2D slices of the film in depth because only light from the focal plane reaches the detector. The Rhodamine B, a common fluorescent agent to dye cells, was used as the fluorescent agent in the PI blend film (Fig. 5a). The immiscible polyimide blend film containing Rhodamine B was prepared from the mixture of PAA2/Rhodamine B and PAA5 solutions in the similar procedure as described for the PI/BN blend film in the experimental section, except that BN filler was replaced with Rhodamine B. The optical morphology of this blend film exhibited the good dispersion of Rhodamine B in the PI2 continuous phase (Fig. 5b). Fig. 5(c) displays the three-dimensional multi-layer fluorescent pattern recordings and the bulk morphology of the 3D fluorescent image formed from the patterns. The images of PI blend film with the orientation of 1–5 layers in $z$-direction were recorded in every 2 μm-steps. In each layer, the fluorescent size was 310 μm × 290 μm. It can be seen that Rhodamine B was activated and emitted fluorescence

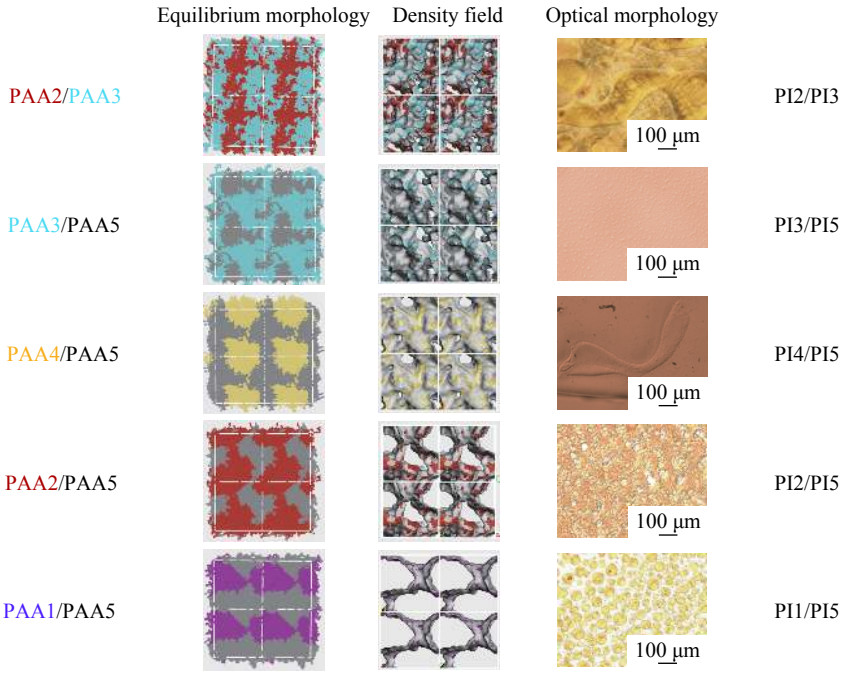


**Fig. 3** Simulation equilibrium morphologies of different PAA blend systems and the optical images of PI films prepared from the corresponding PAA blends

https://doi.org/10.1007/s10118-018-2155-2

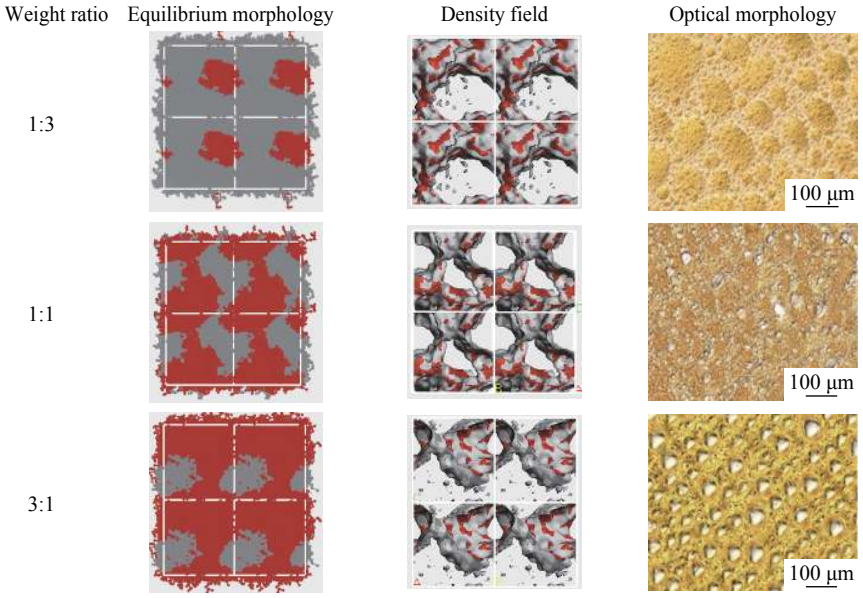


**Fig. 4** Simulation equilibrium morphologies of PAA2/PAA5 blends with different weight ratios and the optical images of PI2/PI5 blend films

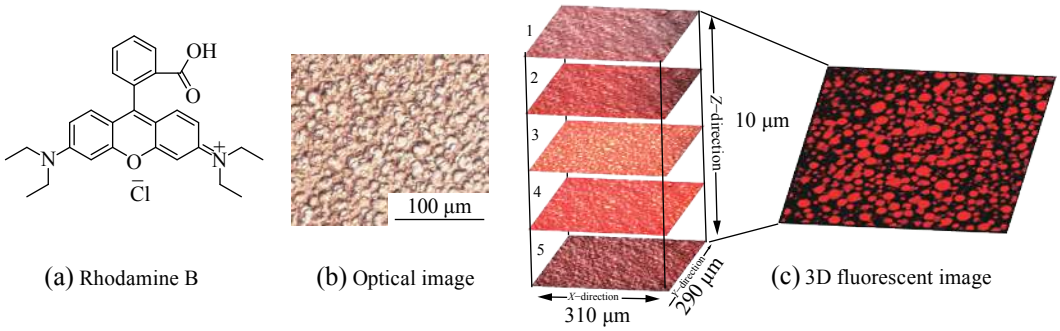


**Fig. 5** The phase separation images of PI2/PI5/Rhodamine B blend film: (a) Chemical structure of Rhodamine B; (b) Optical image of blend film; (c) 3D fluorescent image reconstruction corresponding to the blend film with the orientation of layers 1–5 in the *Z*-direction

only in the existing area. By successive photoirradiation of different layers in the PI blend film, 3D fluorescent image was recorded in the bulk specimen. The fluorescent morphology of blend film also confirmed the formation of phase separation network.

### Mechanical Properties of Polyimide Blend Films

Tensile properties of polyimide blend films prepared from different PAA systems with the weight ratio of 1:1 were evaluated. From the results shown in Fig. 6, it is found that PI3/PI5 blend film exhibited the relatively good mechanical performance with the tensile strength and modulus as high as 159.2 MPa and 5.45 GPa due to the incorporation of rigid TFDB. On the contrary, PI1/PI5 was very brittle with the extremely low tensile strength of 44.7 MPa and elongation at break of 1.15%. The fragility of PI1/PI5 blend film may be related with the existence of rigid PDA and sharp phase separation structure. The other polyimide blend films gave the tensile strength and elongation at break in the range of 80–100 MPa and 3.26%–6.75%, respectively. It is noticed that PI2/PI5 blend film exhibited preferable flexibility due to the presence of flexible ODA structure.

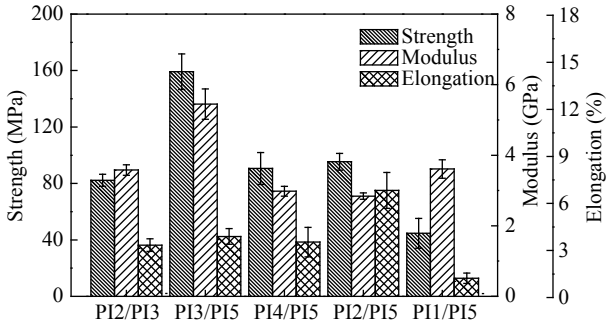


**Fig. 6** Tensile properties of polyimide blend films prepared from different PAA systems

### Morphology of Polyimide/BN Blend Films

In consideration of the good balance of separating ability and mechanical property, PI2/PI5 blend was selected as the matrix to prepare the immiscible polyimide composite films containing BN filler. The correlation of morphology and thermal conductivity of PI2/PI5/BN blend films was

https://doi.org/10.1007/s10118-018-2155-2

investigated and compared with that of the corresponding PI2/BN films. The nano BN was prepared in a different way from micro BN. Generally, the plate-like nano-sized BN fillers are somewhat more polydisperse and favorable to form network, which leads to higher thermal conductivity. However, nano-sized fillers have high interfacial area, which inevitably increases thermal interfacial resistance. The effect of filler size on thermal conductivity of composites, in particular when particle size is in the nanoscale, is still controversial[32]. Therefore, we also discussed the size effect of BN fillers on the thermal conductivity of immiscible polyimide blend films.

The morphologies of PI2/PI5/BN blend films and PI2/BN films with different contents of nano-sized or micro-sized BN were observed by optical microscopy. As shown in Table 3, the PI2/PI5/BN blend films showed a microphase separation structure, which consisted of a continuous BN-rich phase (PI2, dark region) and a BN-poor phase (PI5, bright region). The BN-rich phase became darker with the incorporation of BN filler, while the BN-poor phase was still maintained. It was suggested that the highly connected thermally conductive pathway was formed in the immiscible PI2/PI5/BN blend films. There is no large particle cluster or aggregate of nBN or mBN particles detected for the blended films even when the filler content increased to 25 wt%. On the other hand, the PI2/BN films showed a homogenous morphology, in which the BN fillers (black spots) individually dispersed in the polyimide matrix. It was also found that the nano-sized BN particles were still uniformly dispersed in PI2 matrix with the BN content increasing, whereas the micro-sized BN particles became larger because of the aggregation.

The cross-section of PI2/PI5/nBN blend film containing 25 wt% nano-sized BN was investigated by SEM micrographs. As shown in Fig. 7(a), the brighter regions corresponding to BN-rich phase and the dark region corresponding to BN-poor phase were clearly observed. Moreover, the magnified SEM micrographs of the BN-rich phase and BN-poor phase exhibited a rough morphology for the former and a smooth morphology for the latter (Figs. 7c and 7d). As a comparison, the PI2/mBN film with 25 wt% filler exhibited a uniform structure.

The Raman spectroscopic analysis of PI2/PI5/nBN blend film with 15 wt% nBN was carried out in order to get details of chemical composition. In the confocal Raman microscopy (Fig. 8a), a continuous bright region (I) due to the BN-rich phase and a separated dark region (II) related to the BN-poor phase were detected. The Raman spectrum of region II

**Table 3** Optical images of polyimide/BN blend films with different filler contents

| BN content (wt%) | PI2/PI5 | | PI2 | |
|---|---|---|---|---|
| | nBN | mBN | nBN | mBN |
| 5 | 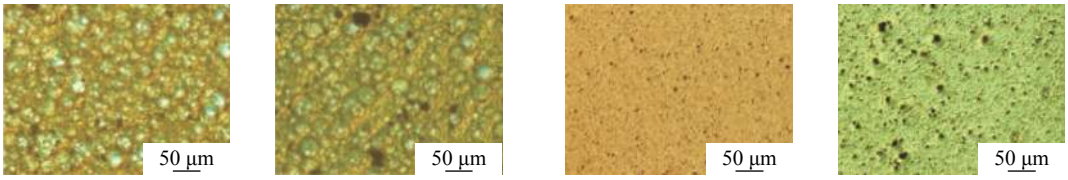 | | | |
| 10 | 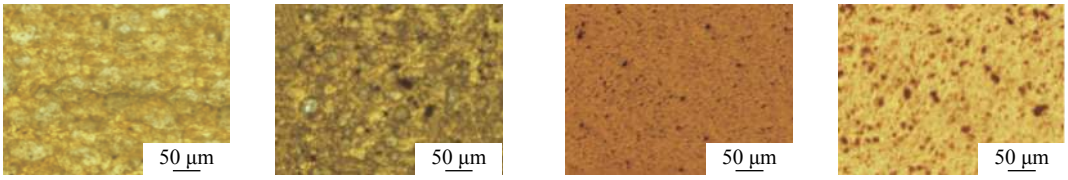 | | | |
| 15 | 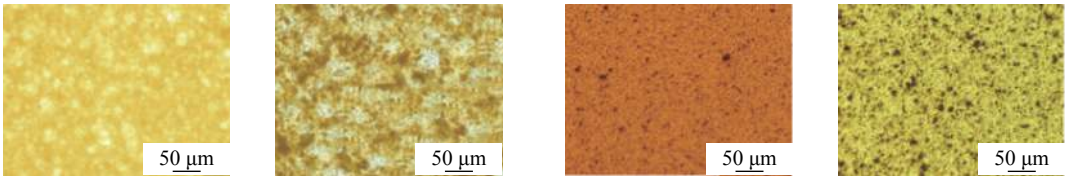 | | | |
| 20 | 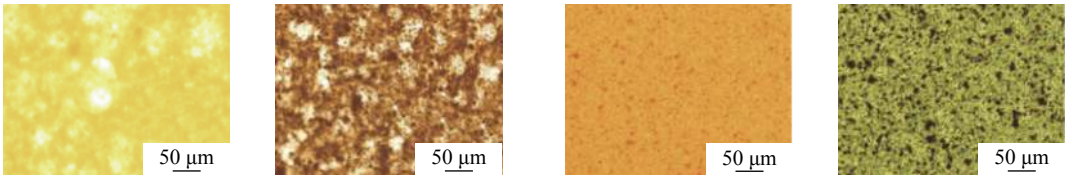 | | | |
| 25 | 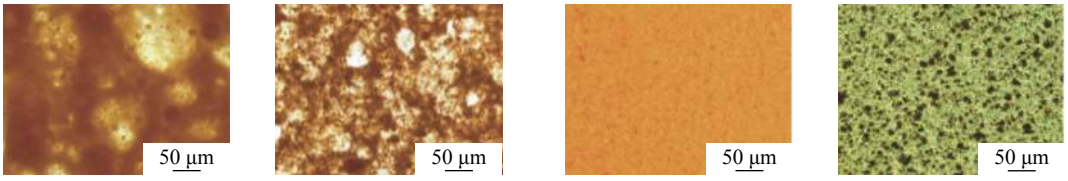 | | | |

https://doi.org/10.1007/s10118-018-2155-2

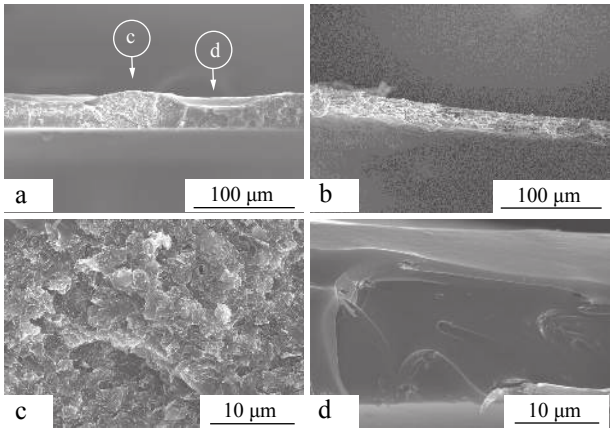


**Fig. 7** SEM micrographs of film cross section: (a) PI2/PI5/nBN blend film with 25 wt% of nBN; (b) PI2/mBN film with 25 wt% of mBN; (c) Magnified BN-rich phase and (d) BN-poor phase in PI2/PI5/nBN

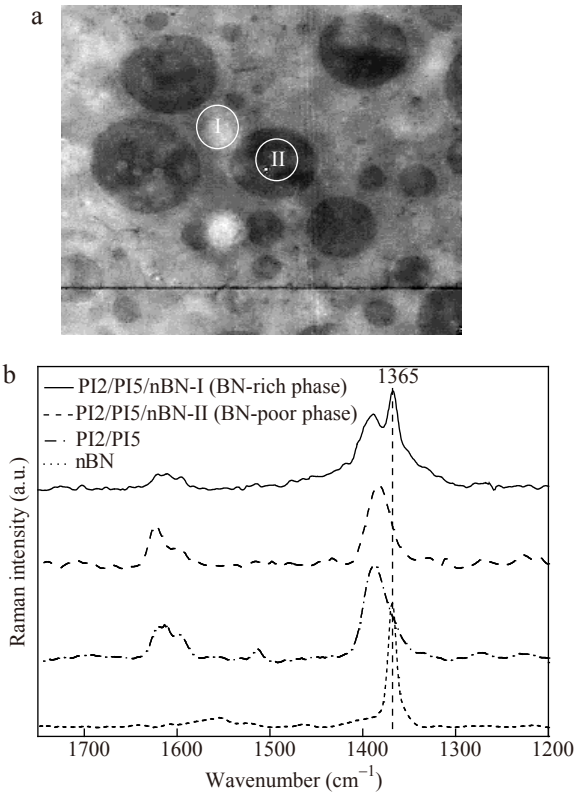


**Fig. 8** Raman spectroscopic analysis of PI2/PI5/nBN blend film with 15 wt% of nBN: (a) Confocal Raman microscopy; (b) Raman spectra of BN-rich phase and BN-poor phase in PI2/PI5/nBN blend films as well as pure PI2/PI5 film and nBN particle

showed no obvious difference with that of neat PI2/PI5 blend film. The characteristic absorptions assigned to the C—N stretching vibration of imide groups and the C=C vibration of phenyl groups were detected around 1379 and 1622 $cm^{-1}$, respectively, implying no existence of nBN particles in the BN-poor phase. By contrast, a strong signal attributed to the B—N absorption at 1365 $cm^{-1}$ was observed in the Raman spectrum of region I, indicating the presence of BN particles in the BN-rich phase.

A combination of these results clearly suggests the formation of co-continuous separated structures, in which two phase are separately aligned alone the out-of-plane direction to the film plane[18]. This type of phase separation has been designated as "vertical double percolation (VDP) structure", which is an effective thermal conductive pathway.

### Thermal Conductivity and Mechanical Properties of Polyimide/BN Blend Films

The thermal conductivity of immiscible and homogenous PI/BN blend films with different filler contents and particle sizes were evaluated. According to the results shown in Fig. 9, the thermal conductivity of all the PI/BN blend films exhibited an enhancement trend accompanying with the BN content increasing. It was known that the thermally conductive network could be more effectively formed with further increasing mass fraction of BN fillers, followed by a thermal percolation behavior, ascribed to the effective connection between the fillers. The thermally conductive path normally generated when the BN content reached about 30 wt% in polymer matrix films. In the case of homogenous PI2/nBN and PI2/mBN films, they exhibited a gradual increase in thermal conductivity with the BN content raising. There is no significant difference between the PI2/nBN and PI2/mBN, which gave the thermal conductivity values of 0.49 and 0.41 W/(m·K), respectively, for the films with 25 wt% of BN. In contrast, the immiscible PI/BN blend films displayed an abrupt increase in thermal conductivity with the incorporation of BN fillers. PI2/PI5/BN blend films with 25 wt% BN exhibited significantly larger thermal conductivity value compared to the homogenous PI2/BN films. The PI2/PI5/nBN blend film gave the thermal conductivity value of 1.16 W/(m·K), which was 236% of the value for the homogenous PI2/nBN film. The significant improvement in thermal conductivity of immiscible polyimide blend films containing BN fillers was attributed to the existence of vertical double percolation structure, which constructed the effective thermal conductive pathway. As comparing the thermal conductivity of PI2/PI5/nBN and PI2/PI5/mBN blend films with the same filler content, the former exhibited better performance than the latter. This may be related to the good dispersion of nano-sized BN in PI2 phase of blend film.

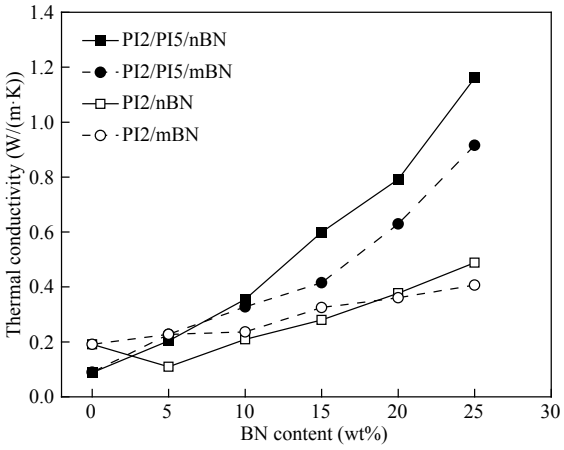


**Fig. 9** Thermal conductivity of PI/BN blend films

https://doi.org/10.1007/s10118-018-2155-2

The tensile properties of immiscible PI/BN blend films with different filler contents and particle sizes were also investigated and are illustrated in Fig. 10. These blend films revealed decline trends in tensile strength and elongation at break with the incorporation of BN. The drop in the tensile properties may be attributed to the relatively weak interface between the polymer matrix and BN particles. However, these PI/BN blend films still displayed reasonable tensile properties even for the film with BN content as high as 25 wt%. The PI2/PI5/nBN and PI2/PI5/mBN films with 25 wt% BN gave the tensile strengths of 49 and 47 MPa, respectively. The tensile modulus of these films still kept around 2–3 GPa no matter the changes of filler content and the particle size.

Furthermore, the tensile properties and thermal conductivity were compared between immiscible PI2/PI5/nBN blend films and homogenous PI2/nBN films. According to the results listed in Table 4, it was found that the tensile properties of the immiscible PI2/PI5/nBN blend film with 15 wt% BN were similar to those of homogenous PI2/nBN blend film with 25 wt% BN, whereas the thermal conductivity of the former was 0.60 W/(m·K), which was 125% of the latter. Therefore, these results suggested that immiscible polyimide blend films with good phase separation structure could provide the good combination of thermally conductive and mechanical properties.

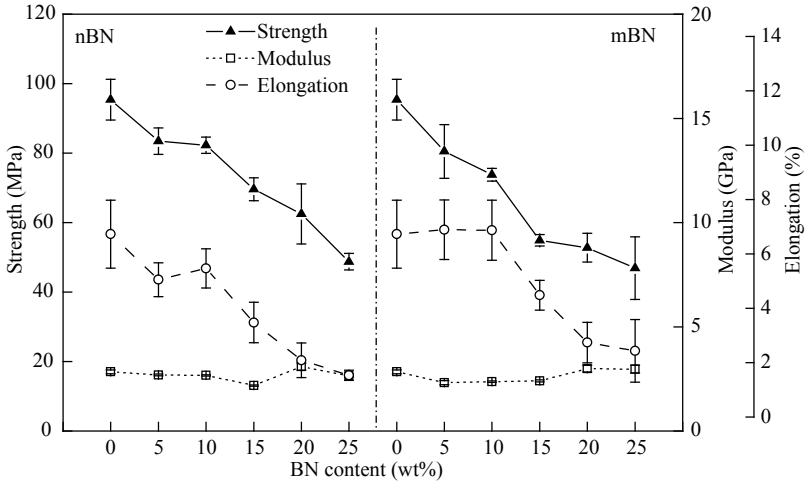


**Fig. 10** Tensile properties of PI2/PI5/nBN and PI2/PI5/mBN blend films with different BN contents

**Table 4** Comparison of tensile properties and thermal conductivity of PI2/PI5/nBN-15wt% and PI2/nBN-25wt% films

| Sample | Tensile strength (MPa) | Tensile modulus (GPa) | Elongation at break (%) | Thermal conductivity (W/(m·K)) |
|---|---|---|---|---|
| PI2/PI5/nBN-15 wt% | 69.6 ± 3.3 | 2.2 ± 0.1 | 3.8 ± 0.7 | 0.60 |
| PI2/nBN-25 wt% | 68.0 ± 5.4 | 2.8 ± 0.1 | 3.8 ± 1.0 | 0.48 |

## CONCLUSIONS

A series of polyamic acids with different Flory-Huggins parameters were selected with the help of mesoscopic simulation. It was found that the PAA blends with high DPD repulsion parameters ($\alpha_{ij}$) were favorable to obtain the films with good phase separation structure. The polyimide blends containing PMDA/ODA and 6FDA/6FAPB with equivalent weight ratio showed good balance between separating ability and mechanical property, which was selected for preparing the polyimide blend films containing BN fillers. The immiscible polyimide blend films revealed better heat dissipation performance than the homogenous polymer films because of the existence of vertical double percolation structure, which constructed the effective thermal conductive pathway. The thermal conductivity for the immiscible PI/BN blend films with 25 wt% nano-sized BN reached as high as 1.16 W/(m·K). The significant enhancement in thermal conductivity was attributed to the good phase separation of polyimide matrix, which made the inorganic fillers selectively localized in one continuous phase with high packing density. It was believed that this simple procedure might provide a facile method to design and fabricate high thermally conductive polyimide composite films with low filler mass fraction.

## ACKNOWLEDGMENTS

We thank Prof. Hongxia Guo and Ms. Chenchen Hu for their helpful discussion. The computational resources for this research are provided by National Supercomputing Center in Shenzhen (Shenzhen Cloud Computing Center).

## REFERENCES

1 Liaw, D. J.; Wang, K. L.; Huang, Y. C.; Lee, K. R.; Lai, J. Y.; Ha, C. S. Advanced polyimide materials: Syntheses, physical properties and applications. Prog. Polym. Sci. 2012, 37(7), 907−974.
2 Tong, H.; Hu, C. C.; Yang, S. Y.; Ma, Y. P.; Guo, H. X.; Fan, L. Preparation of fluorinated polyimides with bulky structure and their gas separation performance correlated with microstructure. Polymer 2015, 69, 138−147.

3 Wen, Y.; Liu, H.; Yang, S. Y.; Fan, L. Transparent and conductive indium tin oxide/polyimide films prepared by high-temperature radio-frequency magnetron sputtering. J. Appl. Polym. Sci. 2015, 132(44), 42753−42764.
4 Chen, H. Y.; Ginzburg, V. V.; Yang, J.; Yang, Y. F.; Liu, W.; Huang, Y.; Du, L. B.; Chen, B. Thermal conductivity of polymer-based composites: Fundamentals and applications. Prog. Polym. Sci. 2016, 59, 41−85.
5 Gu, J. W.; Lv, Z. Y.; Wu, Y. L.; Guo, Y. Q.; Tian, L. D.; Qiu, H.; Li, W. Z.; Zhang, Q. Y. Dielectric thermally conductive boron nitride/polyimide composites with outstanding thermal stabilities *via in-situ* polymerization-electrospinning-hot press method. Compos. Part A-Appl. S. 2017, 94, 209−216.
6 Kuo, D. H.; Lin, C. Y.; Jhou, Y. C.; Cheng, J. Y.; Liou, G. S. Thermal conductive performance of organosoluble polyimide/BN and polyimide/(BN plus AlN) composite films fabricated by a solution-cast method. Polym. Compos. 2013, 34(2), 252−258.
7 Tsai, M. H.; Tseng, I. H.; Chiang, J. C.; Li, J. J. Flexible polyimide films hybrid with functionalized boron nitride and graphene oxide simultaneously to improve thermal conduction and dimensional stability. ACS Appl. Mater. Interfaces 2014, 6(11), 8639−8645.
8 Yu, X. Y.; Qu, X. W.; Naito, K.; Zhang, Q. X. Synthesis, tensile, and thermal properties of polyimide/diamond nanocomposites. J. Reinf. Plast. Compos. 2011, 30(8), 661−670.
9 Li, H. Y.; Ning, S. F.; Hu, H. B.; Bin, L.; Chen, W.; Chen, S. T. Synthesis and electrical properties of polyimide-$Al_2O_3$ composites. Chinese J. Polym. Sci. 2007, 25(3), 271−276.
10 Yu, S.; Lee, J. W.; Han, T. H.; Park, C.; Kwon, Y.; Hong, S. M.; Koo, C. M. Copper shell networks in polymer composites for efficient thermal conduction. ACS Appl. Mater. Interfaces 2013, 5(22), 11618−11622.
11 Choi, S.; Kim, K.; Nam, J.; Shim, S. E. Synthesis of silica-coated graphite by enolization of polyvinylpyrrolidone and its thermal and electrical conductivity in polymer composites. Carbon 2013, 60, 254−265.
12 Li, T. L.; Hsu, S. L. Enhanced thermal conductivity of polyimide films *via* a hybrid of micro- and nano-sized boron nitride. J. Phys. Chem. B 2010, 114(20), 6825−6829.
13 Shoji, Y.; Higashihara, T.; Tokita, M.; Morikawa, J.; Watanabe, J.; Ueda, M. Thermal diffusivity of hexagonal boron nitride composites based on cross-linked liquid crystalline polyimides. ACS Appl. Mater. Interfaces 2013, 5(8), 3417−3423.
14 Murakami, T.; Ebisawa, K.; Miyao, K.; Ando, S. Enhanced thermal conductivity in polyimide/silver particle composite films based on spontaneous formation of thermal conductive paths. J. Photopolym. Sci. Technol. 2014, 27(2), 187−191.
15 Cao, J. P.; Zhao, X.; Zhao, J.; Zha, J. W.; Hu, G. H.; Dang, Z. M. Improved thermal conductivity and flame retardancy in polystyrene/poly(vinylidene fluoride) blends by controlling selective localization and surface modification of SiC nanoparticles. ACS Appl. Mater. Interfaces 2013, 5(15), 6915−6924.
16 Yuan, D. B.; Gao, Y. F.; Guo, Z. X.; Yu, J. Improved thermal conductivity of ceramic filler-filled polyamide composites by using PA6/PA66 1:1 blend as matrix. J. Appl. Polym. Sci. 2017, 134(40), 45371−45377.
17 Yorifuji, D.; Ando, S. Enhanced thermal conductivity over percolation threshold in polyimide blend films containing ZnO nano-pyramidal particles: Advantage of vertical double percolation structure. J. Mater. Chem. 2011, 21(12), 4402−4407.
18 Yorifuji, D.; Ando, S. Enhanced thermal diffusivity by vertical double percolation structures in polyimide blend films containing silver nano particles. Macromol. Chem. Phys. 2010, 211(19), 2118−2124.
19 Sato, K.; Horibe, H.; Shirai, T.; Hotta, Y.; Nakano, H.; Nagai, H.; Mitsuishi, K.; Watari, K. Thermally conductive composite films of hexagonal boron nitride and polyimide with affinity-enhanced interfaces. J. Mater. Chem. 2010, 20(14), 2749−2752.
20 Tanimoto, M.; Yamagata, T.; Miyata, K.; Ando, S. Anisotropic thermal diffusivity of hexagonal boron nitride-filled polyimide films: Effects of filler particle size, aggregation, orientation, and polymer chain rigidity. ACS Appl. Mater. Interfaces 2013, 5(10), 4374−4382.
21 Zhou, W.; Zuo, J.; Zhang, X.; Zhou, A. Thermal, electrical, and mechanical properties of hexagonal boron nitride-reinforced epoxy composites. J. Compos. Mater. 2013, 48(20), 2517−2526.
22 Wang, C.; Paddison, S. J. Mesoscale modeling of hydrated morphologies of sulfonated polysulfone ionomers. Soft Matter 2014, 10(6), 819−830.
23 Zhong, T. P.; Ai, P. F.; Zhou, J. Structures and properties of pamam dendrimer: A multi-scale simulation study. Fluid Phase Equilib. 2011, 302(1-2), 43−47.
24 Xue, Z. J.; Liu, X. Y.; Zhuang, Q. X.; Hu, K.; Han, Z. W. Molecular simulation of the effect of graft structure on the miscibility of high-impact polystyrene blends. Polym. Compos. 2012, 33(3), 430−435.
25 Yu, G.; Liu, J.; Zhou, J. Mesoscopic coarse-grained simulations of lysozyme adsorption. J. Phys. Chem. B 2014, 118(17), 4451−4460.
26 Zhuang, Q. X.; Xue, Z. J.; Liu, X. Y.; Yuan, Y. L.; Han, Z. W. Molecular simulation of miscibility of poly(2,6-dimethyl-1,4-phenylene ether)/poly(styrene-*co*-acrylonitrile) blend with the compatibilizer triblock terpolymer sbm. Polym. Compos. 2011, 32(10), 1671−1680.
27 Chen, H. Y.; Wu, J. H.; Luo, S. J.; Xi, H. X.; Qian, Y. Mesodyn and experimental approach to the structural fabrication and pore-size adjustment of SBA-15 molecular sieves. Adsorpt. Sci. Technol. 2009, 27(6), 579−592.
28 Luo, X.; Xie, S. J.; Huang, W.; Dai, B. N.; Lu, Z. Y.; Yan, D. Y. Effect of branching architecture on glass transition behavior of hyperbranched copolystyrenes: The experiment and simulation studies. Chinese J. Polym. Sci. 2015, 34(1), 77−87.
29 Ouyang, Y. T.; Guo, H. X. Phase behavior of amphiphiles at liquid crystals/water interface: A coarse-grained molecular dynamics study. Chinese J. Polym. Sci. 2014, 32(10), 1298−1310.
30 Tanaka, T.; Yamaguchi, K.; Yamamoto, S. Rhodamine-B-doped and Au(III)-doped PMMA film for three-dimensional multi-layered optical memory. Opt. Commun. 2002, 212(1-3), 45−50.
31 Kumacheva, E.; Kalinina, O.; Lilge, L. Three-dimensional arrays in polymer nanocomposites. Adv. Mater. 1999, 11(3), 231−234.
32 Chen, H.; Ginzburg, V.; Yang, J.; Yang, Y. F.; Liu, W.; Huang, Y.; Du, L. B.; Chen, B. Thermal conductivity of polymer-based composites: Fundamentals and applications. Prog. Polym. Sci. 2016, 59, 41−85.


https://doi.org/10.1007/s10118-018-2155-2